Circuit Implementation of Synchronized Chaos with Applications to Communications

Kevin M. Cuomo and Alan V. Oppenheim
Research Laboratory of Electronics, Massachusetts Institute of Technology, Cambridge, Massachusetts 02139
(Received 21 January 1993)

An analog circuit implementation of the chaotic Lorenz system is described and used to demonstrate two possible approaches to private communications based on synchronized chaotic systems.

PACS numbers: 05.45.+b, 43.72.+q, 84.30.Wp

In 1990 Pecora and Carroll [1] reported that certain chaotic systems possess a self-synchronization property. A chaotic system is self-synchronizing if it can be decomposed into subsystems: a drive system and a stable response subsystem that synchronize when coupled with a common drive signal [1–3]. They showed numerically that synchronization occurs if all of the Lyapunov exponents for the response subsystems are negative. For some synchronizing chaotic systems the ability to synchronize is robust. For example, the Lorenz system is decomposable into two separate response subsystems that will each synchronize to the drive system when started from any initial condition. As discussed in [4–6], the combination of synchronization and unpredictability from purely deterministic systems leads to some potentially interesting communications applications. In this Letter, we focus on the synchronizing properties of the Lorenz system, the implementation of the Lorenz system as an analog circuit, and the potential for utilizing the Lorenz circuit for various communications applications. It should be stressed that the applications indicated are very preliminary and presented primarily to suggest and illustrate possible directions.

The Lorenz system [7] is given by

$$\begin{aligned} \dot{x} &= \sigma(y-x), \\ \dot{y} &= rx - y - xz, \\ \dot{z} &= xy - bz, \end{aligned} \tag{1}$$

where σ, r, and b are parameters. As shown by Pecora and Carroll an interesting property of (1) is that it is decomposable into two stable subsystems. Specifically, a stable (x_1,z_1) response subsystem can be defined by

$$\begin{aligned} \dot{x}_1 &= \sigma(y-x_1), \\ \dot{z}_1 &= x_1 y - bz_1, \end{aligned} \tag{2}$$

and a second stable (y_2,z_2) response subsystem by

$$\begin{aligned} \dot{y}_2 &= rx - y_2 - xz_2, \\ \dot{z}_2 &= xy_2 - bz_2. \end{aligned} \tag{3}$$

Equation (1) can be interpreted as the drive system since its dynamics are independent of the response subsystems. Equations (2) and (3) represent dynamical response systems which are driven by the drive signals $y(t)$ and $x(t)$, respectively. The eigenvalues of the Jacobian matrix for the (x_1,z_1) subsystem are both negative and thus $|x_1-x|$ and $|z_1-z| \to 0$ as $t \to \infty$. Also, it can be shown numerically that the Lyapunov exponents of the (y_2,z_2) subsystem are both negative and thus $|y_2-y|$ and $|z_2-z| \to 0$ as $t \to \infty$.

As we show below, the two response subsystems can be used together to regenerate the full-dimensional dynamics which are evolving at the drive system. Specifically, if the input signal to the (y_2,z_2) subsystem is $x(t)$, then the output $y_2(t)$ can be used to drive the (x_1,z_1) subsystem and subsequently generate a "new" $x(t)$ in addition to having obtained, through synchronization, $y(t)$ and $z(t)$. It is important to recognize that the two response subsystems given by Eqs. (2) and (3) can be combined into a single system having a three-dimensional state space. This produces a full-dimensional response system which is structurally similar to the drive system (1). Further discussion of this result is given below in the context of the circuit implementations.

A direct implementation of Eq. (1) with an electronic circuit presents several difficulties. For example, the state variables in Eq. (1) occupy a wide dynamic range with values that exceed reasonable power supply limits. However, this difficulty can be eliminated by a simple transformation of variables. Specifically, we define new variables by $u = x/10$, $v = y/10$, and $w = z/20$. With this scaling, the Lorenz equations are transformed to

$$\begin{aligned} \dot{u} &= \sigma(v-u), \\ \dot{v} &= ru - v - 20uw, \\ \dot{w} &= 5uv - bw. \end{aligned} \tag{4}$$

This system, which we refer to as the transmitter, can be more easily implemented with an electronic circuit because the state variables all have similar dynamic range and circuit voltages remain well within the range of typical power supply limits.

An analog circuit implementation of the circuit Eqs. (4) is shown in Fig. 1. The operational amplifiers (1–8) and associated circuitry perform the operations of addition, subtraction, and integration. Analog multipliers implement the nonlinear terms in the circuit equations. We emphasize that our circuit implementation of (4) is exact,

0031-9007/93/71(1)/65(4)$06.00

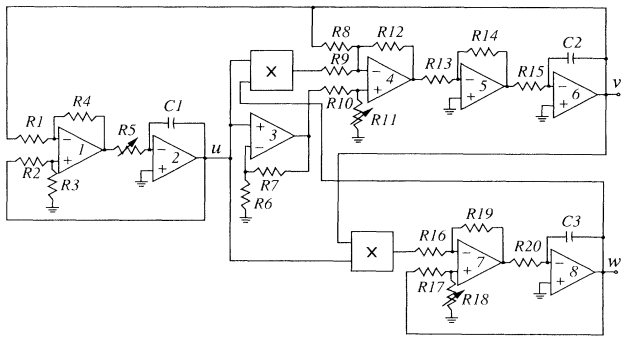

FIG. 1. Lorenz-based chaotic circuit.

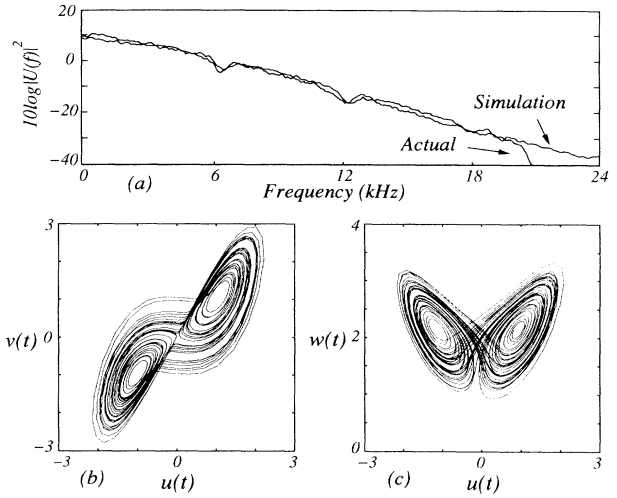

FIG. 2. Circuit data: (a) averaged power spectrum of $u(t)$; (b) chaotic attractor projected onto the uv plane; (c) chaotic attractor projected onto the uw plane.

and that the coefficients σ, r, and b can be independently varied by adjusting the corresponding resistors R_5, R_{11}, and R_{18}. In addition, the circuit time scale can be easily adjusted by changing the values of the three capacitors, C_1, C_2, and C_3, by a common factor. We have chosen component values [Resistors (kΩ): R_1,R_2,R_3,R_4,R_6,R_7, $R_{13},R_{14},R_{16},R_{17},R_{19}=100$; $R_5,R_{10}=49.9$; $R_8=200$; R_9, $R_{12}=10$; $R_{11}=63.4$; $R_{15}=40.2$; $R_{18}=66.5$; $R_{20}=158$; capacitors (pF): $C_1,C_2,C_3=500$ Op-Amps (1-8): LF353 multipliers: AD632AD] which result in the coefficients $\sigma=16$, $r=45.6$, and $b=4$.

To illustrate the chaotic behavior of the transmitter circuit, an analog-to-digital (A/D) data recording system was used to sample the appropriate circuit outputs at a 48-kHz rate and with 16-bit resolution. Figure 2(a) shows the averaged power spectrum of the circuit wave form $u(t)$. The power spectrum is broadband which is typical of a chaotic signal. Figure 2(a) also shows a power spectrum obtained from a numerical simulation of the circuit equations. As we see, the performance of the circuit and the simulation are consistent. Figures 2(b) and 2(c) show the circuit's chaotic attractor projected onto the uv plane and uw plane, respectively. These data were obtained from the circuit using the stereo recording capability of the A/D system to simultaneously sample the x-axis and y-axis signals at a 48-kHz rate and with 16-bit resolution. A more detailed analysis of the transmitter circuit is given in [6].

A full-dimensional response system which will synchronize to the chaotic signals at the transmitter (4) is given by

$$\begin{aligned} \dot{u}_r &= \sigma(v_r - u_r)\,, \\ \dot{v}_r &= ru - v_r - 20uw_r\,, \\ \dot{w}_r &= 5uv_r - bw_r\,. \end{aligned} \tag{5}$$

We refer to this system as the receiver in light of some potential communications applications. We denote the transmitter state variables collectively by the vector $\mathbf{d}=(u,v,w)$ and the receiver variables by the vector $\mathbf{r}=(u_r,v_r,w_r)$ when convenient.

By defining the dynamical errors by $\mathbf{e}=\mathbf{d}-\mathbf{r}$, it is straightforward to show that synchronization in the Lorenz system is a result of stable error dynamics between the transmitter and receiver. Assuming that the transmitter and receiver coefficients are identical, a set of equations which govern the error dynamics are given by

$$\begin{aligned} \dot{e}_1 &= \sigma(e_2 - e_1)\,, \\ \dot{e}_2 &= -e_2 - 20u(t)e_3\,, \\ \dot{e}_3 &= 5u(t)e_2 - be_3\,. \end{aligned}$$

The error dynamics are globally asymptotically stable at the origin provided that $\sigma,b>0$. This result follows by considering the three-dimensional Lyapunov function defined by $E(\mathbf{e},t)=\frac{1}{2}[(1/\sigma)e_1^2+e_2^2+4e_3^2]$. The time rate of change of $E(\mathbf{e},t)$ along trajectories is given by

$$\begin{aligned} \dot{E}(\mathbf{e},t) &= (1/\sigma)e_1\dot{e}_1 + e_2\dot{e}_2 + 4e_3\dot{e}_3 \\ &= -(e_1 - \tfrac{1}{2}e_2)^2 - \tfrac{3}{4}e_2^2 - 4be_3^2\,, \end{aligned}$$

which shows that $E(\mathbf{e},t)$ decreases for all $\mathbf{e}\neq 0$. As $E(\mathbf{e},t)$ goes to zero synchronization occurs. Note that the transmitter and receiver need not be operating chaotically for synchronization to occur. In [8], a similar Lyapunov argument is given for the synchronization of the (y,z) subsystem of the Lorenz equations.

A comparison of the receiver equations (5) with the transmitter equations (4) shows that they are nearly identical, except that the drive signal $u(t)$ replaces the receiver signal $u_r(t)$ in the $(\dot{v}_r,\dot{w}_r)$ equations. This similarity allows the transmitter and receiver circuits to be built in an identical way, which helps to achieve perfect synchronization between the transmitter and receiver. In [6] we discuss and illustrate the synchronization performance of the receiver circuit.

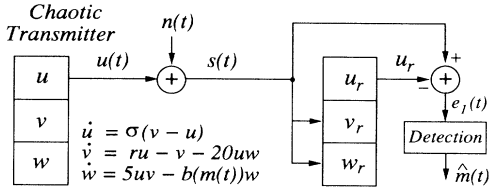

FIG. 3. Chaotic communication system.

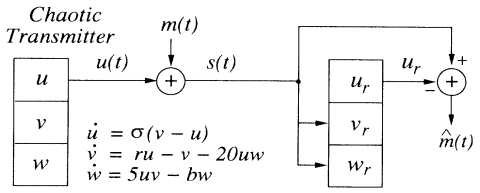

FIG. 5. Chaotic signal masking system.

As one illustration of the potential use of synchronized chaotic systems in communications, we describe a system to transmit and recover binary-valued bit streams [6]. The basic idea is to modulate a transmitter coefficient with the information-bearing wave form and to transmit the chaotic drive signal. At the receiver, the coefficient modulation will produce a synchronization error between the received drive signal and the receiver's regenerated drive signal with an error signal amplitude that depends on the modulation. Using the synchronization error the modulation can be detected.

The modulation/detection process is illustrated in Fig. 3. In this figure, the coefficient b of the transmitter equations (4) is modulated by the information-bearing wave form, $m(t)$. For purposes of demonstrating the technique, we use a square wave for $m(t)$ as illustrated in Fig. 4(a). The square wave produces a variation in the transmitter coefficient b with the zero-bit and one-bit coefficients corresponding to $b(0)=4$ and $b(1)=4.4$, respectively. In [6] we show that the averaged power spectrum of the drive signal with and without the embedded square wave present are very similar. Figure 4(b) shows the synchronization error power, $e_1^2(t)$, at the output of the receiver circuit. The coefficient modulation produces significant synchronization error during a "1" transmission and very little error during a "0" transmission. Figure 4(c) illustrates that the square-wave modulation can be reliably recovered by low pass filtering the synchronization error power wave form and applying a threshold test. This approach has also been shown to work using Chua's circuit [9].

Another potential approach to communications applications is based on signal masking and recovery. In signal masking, a noiselike masking signal is added at the transmitter to the information-bearing signal $m(t)$ and at the receiver the masking is removed. In our system, the basic idea is to use the received signal to regenerate the masking signal at the receiver and subtract it from the received signal to recover $m(t)$. This can be done with the synchronizing receiver circuit since the ability to synchronize is robust, i.e., is not highly sensitive to perturbations in the drive signal and thus can be done with the masked signal. It is interesting to note that this idea is not restricted to just the Lorenz circuit but has wider potential; for example, Kocarev *et al.* [10] have also demonstrated our signal masking concept in [4,5] using Chua's circuit. While there are many possible variations, consider, for example, a transmitted signal of the form $s(t) = u(t) + m(t)$. It is assumed that for masking, the power

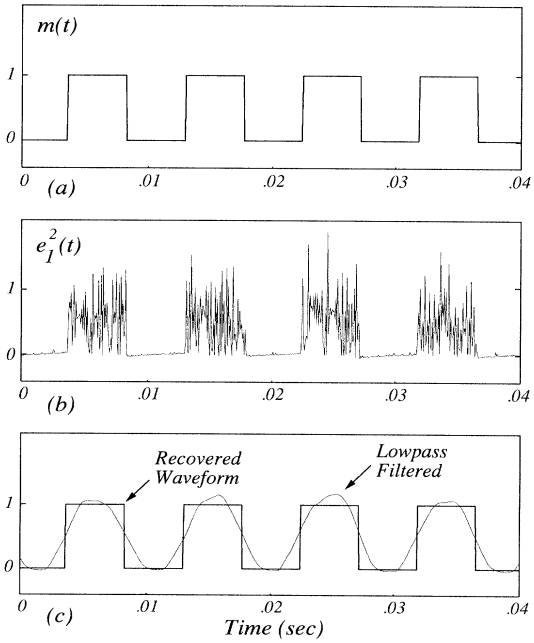

FIG. 4. Circuit data: (a) modulation wave form; (b) synchronization error power; (c) recovered wave form.

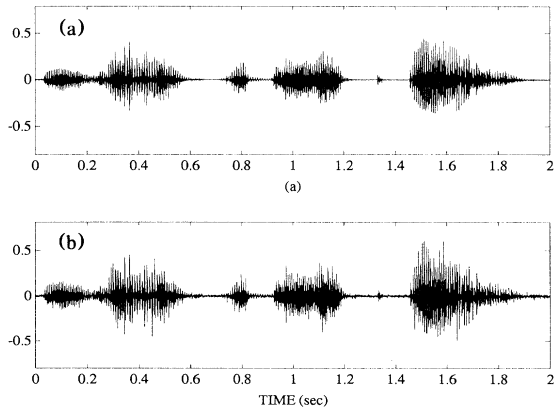

FIG. 6. Circuit data: speech wave forms. (a) Original; (b) recovered.

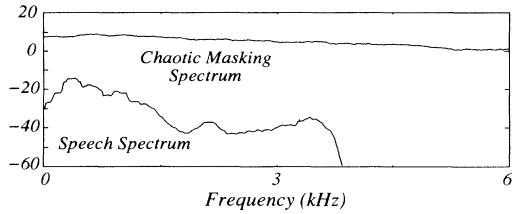

FIG. 7. Circuit data: power spectra of chaotic masking and speech signals.

level of $m(t)$ is significantly lower than that of $u(t)$. The dynamical system implemented at the receiver is

$$\dot{u}_r = 16(v_r - u_r),$$

$$\dot{v}_r = 45.6s(t) - v_r - 20s(t)w_r,$$

$$\dot{w}_r = 5s(t)v_r - 4w_r.$$

If the receiver has synchronized with $s(t)$ as the drive, then $u_r(t) \simeq u(t)$ and consequently $m(t)$ is recovered as $\hat{m}(t) = s(t) - u_r(t)$. Figure 5 illustrates the approach.

Using the transmitter and receiver circuits, we demonstrate the performance of this system in Fig. 6 with a segment of speech from the sentence "He has the bluest eyes." As indicated in Fig. 7 the power spectra of the chaotic masking signal, $u(t)$, and the speech are highly overlapping with an average signal-to-masking ratio of approximately -20 dB. Figures 6(a) and 6(b) show the original speech, $m(t)$, and the recovered speech signal, $\hat{m}(t)$, respectively. Clearly, the speech signal has been recovered and in informal listening tests is of reasonable quality.

We thank S. Isabelle and S. Strogatz for helpful discussions. This work was sponsored in part by the Air Force Office of Scientific Research under Grant No. AFOSR-91-0034-A, in part by a subcontract from Lockheed Sanders, Inc., under ONR Contract No. N00014-91-C-0125, and in part by the Defense Advanced Research Projects Agency monitored by the Office of Naval Research under Grant No. N00014-89-J-1489. K.M.C. is supported in part through the MIT/Lincoln Laboratory Staff Associate Program.

[1] L. M. Pecora and T. L. Carroll, Phys. Rev. Lett. **64**, 821 (1990).
[2] T. L. Carroll and L. M. Pecora, IEEE Trans. Circuits Syst. **38**, 453 (1991).
[3] L. M. Pecora and T. L. Carroll, Phys. Rev. A **44**, 2374 (1991).
[4] K. M. Cuomo, A. V. Oppenheim, and S. H. Isabelle, MIT Research Laboratory of Electronics TR No. 570, 1992 (unpublished).
[5] A. V. Oppenheim, G. W. Wornell, S. H. Isabelle, and K. M. Cuomo, in Proceedings of the IEEE International Conference on Acoustics, Speech, and Signal Processing, 1992 (to be published).
[6] K. M. Cuomo and A. V. Oppenheim, MIT Research Laboratory of Electronics TR No. 575, 1992 (unpublished).
[7] E. N. Lorenz, J. Atmos. Sci. **20**, 130 (1963).
[8] R. He and P. G. Vaidya, Phys. Rev. A **46**, 7387 (1992).
[9] U. Parlitz, L. Chua, Lj. Kocarev, K. Halle, and A. Shang, Int. J. Bif. Chaos **2**, 973 (1992).
[10] Lj. Kocarev, K. Halle, K. Eckert, and L. Chua, Int. J. Bif. Chaos **2**, 709 (1992).